2-1-2016

Design Live Load Factor Calibration for Michigan Highway Bridges

Christopher D. Eamon
Wayne State University, eamon@eng.wayne.edu

Valid Kamjoo
Wayne State University

Kazuhiko Shinki
Wayne State University

Design Live Load Factor Calibration for Michigan Highway Bridges

Christopher D. Eamon[1], Valid Kamjoo[2], and Kazuhiko Shinki[3]

Abstract

In this study, a reliability-based calibration of live load factors for bridge design specific to the State of Michigan was conducted. Two years of high frequency WIM data from 20 representative state-wide sites were analyzed, and load effects were generated for bridge spans from 6 to 122 m (20 to 400 ft), considering simple and continuous moments and shears, as well as single lane and two lane effects. Seventy-five year statistics for maximum live load were then estimated with probabilistic projection. Bridge girders considered for the calibration included composite steel, prestressed concrete, side-by-side and spread box beams, as well as special long span structural members. In some cases, it was found that Michigan load effects are greater than those previously assumed, often requiring higher load factors than in current use. Moreover, significant variation in the required load factor was found, potentially resulting significant inconsistencies in reliability if a single load factor is used for the design of all bridge types and load effects considered.

---

1. Associate Professor of Civil and Environmental Engineering, Wayne State University, Detroit, MI 48202; eamon@eng.wayne.edu.
2. PhD Candidate, Dept. of Civil and Environmental Engineering, Wayne State University.
3. Assistant Professor of Mathematics, Wayne State University.

Introduction

In 1994, the 1st Edition of the AASHTO LRFD Bridge Design Specifications was published (AASHTO 1994), with the intent to provide a consistent level of reliability to bridge structures by using the probabilistically-calibrated Load and Resistance Factor Design (LRFD) format. Due to the limited amount of traffic data available at the time, the LRFD load model was developed from a sample of approximately 9,000 trucks surveyed in Ontario in 1975. The Ontario survey was biased as the surveyors mostly weighed trucks that showed signs of carrying heavy loads. Moreover, several assumptions were made to allow extrapolation of the data to the 75-year expected maximum load statistics used for calibration. For example, it was assumed that every 15th heavy truck was side-by-side with another, where a heavy truck was taken from the biased truck sample. It was also assumed that every 30 side-by-side truck events occur with fully correlated (i.e. identical) truck weights. Using these and other load statistics for reliability assessment led to the development of the HL-93 design load with live load factor of 1.75 and associated adjustment factors, to meet a target reliability level for LRFD design set at β=3.5. Bridges with spans greater than 61 m (200 ft) were not considered (Nowak 1999).

Over the last two decades, several DOTs have began work to re-calibrate the AASHTO live load factors for design as well as rating to better represent state-specific traffic loads collected from weigh-in-motion (WIM) devices. For example, the Texas Department of Transportation developed a procedure to determine equivalent single axle loads from WIM-collected traffic information (Lee and Souny-Slitine 1998), while Wisconsin DOT modeled maximum load effects from WIM data by fitting multi-modal distributions to axle loads and spacings, then using Monte Carlo Simulation (MCS) to model the axle load and spacing relationships (Tatabai et al. 2009). Similarly, Missouri and Oregon DOTs completed a

recalibration of live load factors for bridge design and rating based on local WIM data (Kwon et. al. 2010; Pelphery et al. 2006), and Ghosn et al. (2011) used the adjustment procedure presented in the AASHTO Manual for Bridge Evaluation (MBE) (AASHTO 2011) to develop a load and resistance factor rating method for permit and legal loads for New York State DOT.

The popularity of this effort is recognized in the publication of NCHRP Report 683 (Sivakumar et al. 2011) which offers specific recommendations to conduct live load factor recalibration. In addition, various other sources provide recommendations for WIM data filtering and validation (FHWA 2001; Pelphrey and Higgins 2006; Tabatabai et al. 2009; O'Brien and Enright 2011). Other efforts include those of Raz et al. (2004), who proposed a data mining approach for automatically detecting anomalies in WIM data, and Monsere et al. (2008), who studied methods for collecting, sorting, filtering, and archiving WIM data to facilitate development of high-quality long-term records. When insufficient data are available, as well as to enhance the accuracy of load effect projections to longer periods of time needed for design and rating, some have used simulation methods to extend the data pool (Bruls et al. 1996; O'Connor et al. 2001; Croce and Salvatore 2001; O'Brien and Caparani 2005; Gindy and Nassif 2006; Sivakumar et al. 2011; O'Brien and Enright 2010, 2011).

In the State of Michigan, in response to the unusually heavy legal loads allowed, described in more detail below, as early as 1973, the Michigan Department of Transportation (MDOT) increased its design load beyond the HS20 standard to HS25 (MDOT 2009). Later, as precursors to this study, a series of research efforts were conducted to better characterize Michigan traffic loads (Van de Lindt and Fu 2002; Fu and Van de Lindt 2006; Curtis and Till 2008). Although valuable, due to limitations of data availability, this previous work was based on non-high speed WIM data, from which no following or side-by-side vehicle configurations

could be directly measured, a small number of WIM sites, a small selection of bridges, as well as other approximations in converting WIM data to load effects. The most recent effort (Curtis and Till 2008) resulted in a design load change that is currently in use by MDOT, *HL93-mod*. This design load was an indirect result of updating the bridge rating procedure, where the method outlined in NCHRP 454 (Moses 2001) was used to estimate appropriate live load factors for heavy legal and permit vehicles. However, use of this procedure resulted in load factors that would cause the operational capacity of bridges designed under LRFD with HL-93 to be restricted from carrying common overload permit vehicles in Michigan. Therefore, the design load was increased until new bridges could carry these frequent permit vehicles (referred to as "Class A" overloads). This HL93-mod design load consists of replacing the LRFD 110 kN (25 kip) tandem load with a single 270 (60 kip) axle, as well as an additional factor of 1.2 that is applied to the existing LRFD live load factor of 1.75. The resulting equivalent load factor that would be applied to a HL-93 load effect was exceptionally high in some cases, from approximately 2.1-3.6, depending on span length, where the highest effective factors result on the shorter spans.

When evaluating the effect of this increased design load, however, in conjunction with better WIM data as well as a substantially wider range of bridge geometries than originally considered, it was found that some safety levels were insufficient, where approximately 35% of the 340 types of composite steel girder, prestressed concrete girder, and box-beam structures analyzed, mostly with simple spans from 24-60 m (80-200 ft) (where effective MDOT load factors are lowest), had reliability indices between 2-3, under the desired target of 3.5 (Eamon et al. 2014). Based on collection efforts conducted over the last several years in Michigan, high-quality WIM data recently became available. The purpose of this study is to use these data to

develop Michigan-specific live load factors for the design of highway bridges within the AASHTO LRFD format.

WIM Data

Data from 20 representative WIM stations throughout Michigan were used in this study. These stations collect traffic data at a frequency of 1000 Hz, a sampling rate that can precisely capture the location of vehicles in a group relative to one-another. This allows accurate determination of load effects caused by multiple vehicle presence, a case which typically produces the greatest loads. Of these WIM stations, 16 are on major interstate routes (such as I-94, I-69, I-75, I-96), while four are on lower volume US and intra-state M routes (such as US-127 and M-95). Over the two-year period for which data were collected (in 2011 and 2012), average daily truck traffic (ADTT) ranged from 400 to 11,100, depending on station location, with 10 stations of approximately 5000 ADTT or greater, 3 stations with approximately 2500 ADTT, 5 with approximately 1000 ADTT, and 2 with approximately 400 ADTT.

Data were collected with quartz piezoelectric sensor systems permanently embedded in and flush to the roadway surface. The system consists of the weight sensors, which are approximately 50 mm (2 in) wide units containing cables that span the roadway perpendicular to the traffic direction, and inductive loops (wires laid out in the shape of a large square) also embedded in the roadway. One loop is placed on either side of the sensors. The loop placed before the sensors detects the presence of an oncoming vehicle and activates the WIM system, while the loop placed after the sensors is used to track the time that vehicle axles cross between the loops, information which the system then uses to determine the vehicle speed and axle spacing. Each lane has its own sensor system. The multi-lane systems are linked and time-

stamped to enable recording of vehicle crossing events relative to one-another. For calibrated test vehicles, gauge accuracy was found to be within 10% GVW, and usually within 5% GVW.

Each WIM station employs an automatic filtering system that removes the majority of non-critical traffic from the database. These lightweight vehicles (Classes 1-3) include motorcycles, cars, and light trucks up to 5 axles, with gross vehicle weight (GWV) up to 67 kN (15 kips). WIM stations are consistently monitored and periodically calibrated by MDOT personnel to ensure accuracy. After the automatic filtering was employed, across all sites, there were approximately 92 million total vehicle crossing events recorded for processing in this study.

As WIM data is associated with collection errors (FHWA 2001), after extensive discussions with MDOT personnel, additional data filtering criteria were used to eliminate presumed erroneous records from the database. These additional criteria are summarized in Table 1. A few comments with regard to these criteria are as follows. The WIM system records each axle weight as well as cumulatively sums these as the vehicle travels over the system to calculate GVW. In some cases, there is a discrepancy between these values, indicating a possible bad reading. The data were filtered considering various levels of allowable error, from 1%-10%, and no significant difference in event statistics was found. The axle weight, spacing, and number of axles criteria were chosen based on physical limits of reasonable vehicles found in Michigan, in accordance with recommendations of DOT personnel. Moreover, to reduce bulk of the database, lightweight vehicles were eliminated as noted above, as these have no effect on the load model used in the calibration (as described below) which is governed by heavy vehicle load effects. Vehicle speed is also a consideration, where both low and high speed traffic are associated with data errors. NCHRP 683 (Sivakumar et al. 2011), for example, suggests a lower limit of 16 kph (10 mph). In this study, however, a higher limit of 30 kph (20

mph) was chosen, as MDOT found that a significant number of unreasonable vehicle configurations were being recorded at speeds below this limit. Such presumed erroneous records were found to occur in dense traffic situations when vehicles move slowly and become closely spaced, where the WIM system frequently links the front axle of a following vehicle to the rear axle of the head vehicle. These slow-speed traffic patterns are regarded as a special situation by the DOT and are beyond the scope of this study, as the resulting load effects cannot be accurately measured with the WIM equipment as currently implemented in Michigan. Although significant effort was used to establish appropriate filtering criteria, it is of interest to note that that the resulting vehicle crossing event statistics were not particularly sensitive to reasonable changes in the filtering limits.

Application of the filtering criteria in Table 1 eliminated approximately 30% of the remaining vehicle crossing events to leave 66.3 million events in the database. Most stations had about 30-40% of events eliminated, with a range of about 17-66%. This elimination rate falls within the range of results reported in NCHRP 683 (Sivakumar et al. 2011) from data collected in several other states, for which the elimination rate varied from about 19-74% for different WIM sites (note that in this paper, ADTT refers to that determined from the WIM data before the filtering criteria of Table 1 are applied).

A frequency histogram of the resulting WIM data is shown in Figure 1. As expected, the plot is primarily bi-modal, with peak GVW frequencies at approximately 334 kN (75 kips) and 156 kN (35 kips), which represent the most common loaded and unloaded 5-axle truck weights in Michigan. The maximum truck weight recorded was 2420 kN (543 kips), a special permit vehicle. Note that the figure is truncated at 800 kN GVW, as vehicles with GVW beyond about 700 kN (160 kips) appear so infrequently (relatively) that they are not visible on the figure.

Nearly all sites are represented with similar multi-modal frequency plots, though peaks shift somewhat as a function of differences in local traffic density. However, no particular pattern was found between differences in curve shape and site location or ADTT level.

Figure 2 provides a histogram of the top 5% of GVW, with a peak at approximately 356 kN (80 kips), and another at approximately 600 kN (135 kips). For heavy vehicles (GVW>330 kN (75 kips)), GWV is fairly evenly spread among vehicle lengths from 15-40 m (50-130 ft), with the heaviest vehicles most frequently occurring at lengths between 15-18 m (50-60 ft). As expected, the number and percentage of vehicle crossing events generally decreases as the ratio of (GVW/vehicle length) increases, with most frequent GWV/length ratios for legal vehicles below 356 kN (80 kips) between 7-15 kN/m (0.5-1.0 kip/ft); for legal vehicles above 356 kN between 15-30 kN/m (1.0-2.0 kips/ft); and for non-legal vehicles of all weights, between 15-30 kN/m. To further verify the results, heavy vehicle statistics found from an investigation of the available permit record were compared to those calculated from the WIM data, as well as data checks focused on 5-axle (Class 9 or 3S2) semi-trailer truck data, on a site-by-site basis. These included comparisons of drive tandem axle spacing, drive axle weight, and steering axle weight, which all fell within expected values (Eamon et al. 2014). Based on these multiple verification checks, the collected WIM data were deemed reasonable.

Overall, sites from across the state are similar with regard to typical truck traffic, where approximately 80% of the trucks at all sites are represented by a 3S2 configuration, where average axle weights, spacings, and GVW for the loaded and unloaded vehicles are similar, as described above. For the top 5% of GVW vehicles, most trucks (about 68%) have from 9 to 11 axles, while only about 15% have 5-axles. Some site-specific values for all vehicles recorded and for the top 5% of GVW are shown in Table **2**, where the numerical site label in the table

refers to the corresponding ADTT group. For all vehicles, mean vehicle weight varied among sites from 207-269 kN (47-60 kips), with most sites (10) varying narrowly between 248-255 kN (56-57 kips), and 15 sites between 246-269 kN (55-60 kips). For the top 5% of vehicles, mean GVW varied more significantly, from 360-709 kN (81-159 kips). However, similar to the finding for all vehicles, most sites fall within a relatively narrow range of mean GVW for the top 5%, where 10 sites have values between 518-599 kN (116-134 kips). Moreover, when grouping sites by ADTT level, the average GVW among groups varied only from 245-253 kN (55-57 kips) for all vehicles and from 120-149 kips for the top 5% of vehicles, with no apparent pattern between mean GVW and ADTT present.

As expected, however, the maximum GVW recorded does increase with ADTT level, from an average of 961 kN (216 kips) for the lowest ADTT sites to an average of 1700 kN (382 kips) for the highest ADTT sites. Such an increase can be attributed to the higher likelihood of extreme (high and low) weight vehicles occurring with an increase in traffic volume. Although a significant range exists among sites for the maximum single vehicle weight recorded, from 1120-2420 kN (252-543 kips), the overall profile of maximum vehicle weight is similar, where 10 sites recorded a maximum GVW less than 1300 kN (290 kips) and 16 recorded maximum GVWs less than 1780 kN (400 kips).

Multiple presence probabilities were calculated for vehicles in various spatial configurations, including vehicles following each other in a single lane; vehicles side-by-side in two lanes, and multiple vehicles in both side-by-side and following arrangements. These were calculated for different definitions of multiple presence and vehicle spacing, different ADTT levels, and bridge spans. A brief selection of these results is presented in Tables 3 and 4. Table 3 presents side-by-side probability results for various ADTT levels and ranges of vehicle

headway, defined here as the distance between the front axles of trucks in adjacent lanes. Any two trucks in adjacent lanes with headway less than or equal to that given in the table were counted as side-by-side. Another way side-by-side vehicle overlap is measured in Table 3 is relative to truck length, where trucks are considered side-by-side if headway is less than or equal to half of the vehicle length. This is designated as "1/2 TL" in the table. Table 4 presents multiple presence probabilities for following and multiple groupings. Here, following refers to the presence of two or more vehicles in the same lane when the distance between the trucks is less than or equal to the bridge span, such that at least one axle from each truck is on the span. A multiple case is one in which trucks on the span are in adjacent lanes as well as in the same lane; i.e. a combination of following and side-by-side cases. Note that the results shown in Tables 3 and 4 are based on WIM data that meet the filtering criteria shown in Table 1; it is possible that including all of the WIM data collected (i.e. unfiltered) may alter the values shown.

Overall, it was found that single vehicle passage probability varies from nearly 100% to 91%, depending on span, headway distance, and ADTT. Following events were found to vary from 0.03-8.9%, depending on span and ADTT, while side-by-side probability varies from 0.04-5.6%, depending on headway and ADTT. Finally, multiple was found to vary from 0.02-2.1%, depending on span, ADTT, and headway. As expected, the percentage of following and multiple events increase as span and ADTT level increase. Similarly, the percentage of side-by-side crossings increase as ADTT and allowable vehicle headway increase. For comparison, using an 18 m (60 ft) headway, side-by-side probability was found to be 2.25% for high ADTT levels, while a very similar value (2%) was used in the MBE calibration (Sivakumar et al. 2011). Based on an analysis of data from all sites, the probability of two special permit trucks side-by-side was found to be practically zero. The effect of traffic direction (i.e. vehicles traveling in the same

direction or vehicles traveling in opposing directions) on side-by-side probability for the general truck population was also explored. In general, it was found that traffic direction did not have a consistent nor particularly significant effect on side-by-side probability, where the proportion of side-by-side events with traffic in the same direction (as opposed to events with traffic travelling in the opposite direction) varied from about 44%-53%, depending on site and headway distance considered, with slightly less in the same direction (about 49%) on average. Note that the multiple presence data were not directly used in the design calibration, but are useful for verifying the reasonableness of the WIM data, as well as for a related rating calibration effort that is beyond the scope of this paper (Eamon et al. 2014).

Load Effects

Vehicle load effects were calculated for span lengths from 6-122 m (20-400 ft). Considered effects were maximum simple span moments and shears, and maximum continuous span positive or negative moments and shears, for both single lane and two-lane load cases. These effects were calculated by incrementing the train of measured vehicle configurations and spatial placements (i.e. the actual axle spacing, weights, and vehicle following distances in each lane) recorded from the WIM data across a one-dimensional beam model of the considered span lengths, and recording maximum load effects. When vehicles are present in both lanes, two beam models are used, one for each lane, where the position of vehicles in both lanes are linked in time as they are incremented over the span, such that the total load effect on the span caused by the actual positions of the vehicle group is maintained. To distribute loads to a single girder, the load effect from both lanes are weighted appropriately then summed together using the process described in the Load and Resistance Model section.

A selection of these results is presented in Tables 5 and 6, which summarize load effects, while Figure 3 compares measured to maximum and mean HL93-mod load effects. Note that the load effects shown are for the entire bridge, prior to any reduction due to girder distribution or inclusion of any other factors such as dynamic effect. Also note in Table 4, the "two lane" effects only include results where at least one axle of vehicles in both lanes fit on the given span. As seen, for lower length spans, single lane effects dominate in Michigan, while as the span increases, two lane load effects govern. From Table 5, it can be seen that following vehicle effects are insignificant at spans of 15 m (50 ft) or less, but become very significant at longer spans. From Figure 3, it can be seen that the single maximum load effects found in the WIM data are substantially higher than the HL93-mod (nominal) design load, nearly reaching 3 times the HL93-mod value for moment and shear, although mean load effects are much lower, less than half of the HL93-mod load effect.

Figure 4 presents ratios of the top 5% of moment and shear load effects (which are particularly important for load factor calibration, as discussed below) to the HL93-mod load effect. For comparison, values are taken from sites with lowest load effects ("low"), highest load effects ("high"), and average load effects from all sites. As shown, all load effects tend to sharply increase from 6-15 m (50 ft) spans, then become asymptotic as span further increases. More particularly, 1-lane load effects tend to level off or slightly increase as span increases, while 2-lane effects generally peak close to 31 m (100 ft), then decrease slightly with further increases in span, a trend which holds for moments as well as shears. This is due to the typical governing vehicle combinations for 1-lane and 2-lane load effects, which contribute to producing this pattern. For 1-lane load effects, vehicles with 9 to 11 axles dominate the top 5% of results, as noted above, and as the span increases, the additional load caused by following vehicles

becomes more significant, as shown in Table 6. For 2-lane effects, however, the presence of two 9 to 11 axle trucks in both lanes simultaneously is extremely rare. Rather, the top 5% of 2-lane load effects are dominated by combinations of either two 5 axle trucks or one 9 to 11 axle truck together with a 5 axle truck (one in each lane). These different combinations contribute to the different span-dependent trends shown in the figures. Also note that the 2-lane load effects are greater than 1-lane load effects (prior to the application of distribution factors or other modifications to distribute final load effect to the girder). Although this perhaps appears intuitive, it is not an obvious conclusion before analysis, as the governing trucks that appear on the span in only one lane are generally heavier than either of the governing trucks that appear simultaneously in both lanes, as discussed above. This observation can be seen on the figures by noting the (relatively) small difference between the 1-lane and 2-lane load effects.

Note that the results shown in Figure 4 only vaguely resemble the curves presented in Figure 3. Considering the mean values shown in Figure 3, although the overall trends are similar to those shown in Figure 4, the values of Figure 3 are much lower, as the top 5% of load effects are given in Figure 4 but the entire vehicle pool is considered in Figure 3. Even greater differences can be seen when comparing the single maximum values in Figure 3 to the mean top 5% results shown in Figure 4, as well as when comparing the single maximums in Figure 3 to the overall means shown in Figure 3. This is because the maximum curves are essentially a graph of single outliers, which may occur in no particular pattern, whereas the mean value curves graph the trend of the wider data pool of millions of load effects.

Bridges Considered

The calibration was conducted for two-lane bridges with composite steel and prestressed

concrete (PC) I-girders, as well as PC spread and side-by-side box beams. Both simple span and two-span continuous structures with the above girder types were analyzed, with spans from 6-61 m (20-200 ft) and girder spacing from 1.2-3.6 m (4-12 ft). Bridges were assumed to support a reinforced concrete deck, wearing surface, and additional typical non-structural items (primarily barriers and diaphragms) relevant for dead load calculation. Component dead loads were based on values used in the AASHTO LRFD calibration (Nowak 1999) as well as NCHRP Reports 683 and 285 (Sivakumar et al. 2011; Sivakumar and Ghosn 2011). Per MDOT practice, for design, PC bridges are assumed to act continuous for live load only.

For consideration of spans greater than 61 m (200 ft, where the specific span lengths of 92 m (300 ft) and 122 m (400 ft) were used in this study), girder bridges are not practical for MDOT and special configurations are used, such as trusses and segmental structures with large hollow sections. As these structures are unique and have significantly varying geometries, a general approach was taken that is applicable to any long-span bridge composed of either steel or PC components, which is described in further detail below. It should be noted that load effects on these long spans may be governed by closely spaced, slow moving vehicles, traffic patterns for which the current Michigan WIM sensors cannot accurately capture, as noted above. As such, these structures may require additional consideration as such traffic information becomes available.

Load and Resistance Models

Code calibration is generally conducted separately for Strength I and Strength II limit states, where Strength I is reserved for routine traffic and Strength II concerns special permit vehicles. The traffic loads used in recent AASHTO Strength I calibration efforts included legal

loads, routine permit loads, as well as illegal vehicles that resemble legal and routine vehicle configurations, while Strength II considered special permit vehicles and illegal vehicle configurations resembling special permit vehicles (Sivakumar et al. 2011; Sivakumar and Ghosn 2011). Although the specific definition of a special permit may vary, in this study, a special permit vehicle refers to a non-legal vehicle for which a single passage permit is granted to cross over a specific structure(s), while the vehicle weight and configuration are known with certainty.

In Michigan, however, the appropriateness of separate Strength I and II calibrations is questionable, because the vast majority of special permit load effects are actually enveloped by legal load effects, and the resulting difference between including or excluding above-legal vehicle load effects in the routine traffic data pool was found to be insignificant. This is because Michigan legal vehicle loads are very high (up to 730 kN (164 kips) GVW) and correspondingly, the number of vehicles that exceed the routine permit and legal load effect is very small; approximately 99.99-99.86% of trucks in the WIM database were found to be below the routine permit and legal load effect, depending on span length. Therefore, in this study, a combined Michigan Strength I & II calibration is conducted, and all vehicles from the WIM data are used to generate load effects for the combined calibration, which is conducted for moment and shear limit states.

Here several issues should be noted. First, these results are Michigan-specific. That is, using a different set of load data, such as from another state, may result in significant differences between legal and routine permit only and all-vehicle load effects, particularly if legal load effects are below a substantial number of special permit vehicles. Second, using a different load projection technique to develop the load model than that used in this study (see below) may result in a different sensitivity to the presence of a small number of heavy vehicles. Finally, a

significant number of vehicle permits are granted in Michigan due to exceeding geometric limits or exceptions for individual axle weight or axle spacing, even though the vast majority of these permit vehicles do not exceed the legal load effect.

As a 75-year design lifetime is assumed for design calibration, expected statistics must be projected from the available two-year load effects. In this study, various techniques were considered for extrapolation, including fitting the complete cumulative distribution function of load effects for a site to a trial distribution (Kwon et al. 2010), as well as the use of higher order extreme type curves (Fu and Van de Lindt 2006). However, it was found that these various approaches did not provide significantly better results than the process suggested by Sivakumar et al. (2011), where if the tail end of the data is reasonably normally distributed, an Extreme Type I distribution can be used to extrapolate to future load events. Here, the upper 5% of the load effect data are used for extrapolation. To verify the normality of the tail, a normal probability plot is constructed and a linear regression line with slope (m) and intercept (n) are fit to the plot. A linear trend indicates that the data approach a normal distribution. The mean value of the best-fit normal distribution is then given as: $\bar{x} = -n/m$; with standard deviation $\sigma = \left((1-n)/m\right) - \bar{x}$. The load effect statistics (mean maximum $\bar{L}_{\max}$ and standard deviation $\sigma_{L\max}$) for the projected return period can be computed as follows (Ang and Tang 2007; AASHTO 2011; Sivakumar et al. 2011):

$$\bar{L}_{\max} = \mu_N + \frac{0.5772157}{\alpha_N} \tag{1}$$

$$\sigma_{L\max} = \frac{\pi}{\sqrt{6}\alpha_N} \tag{2}$$

where

$$\mu_N = \bar{x} + \sigma\left(\sqrt{2\ln(N)} - \frac{\ln(\ln(N)) + \ln(4\pi)}{2\sqrt{2\ln(N)}}\right) \quad (3)$$

$$\alpha_N = \frac{\sqrt{2\ln(N)}}{\sigma} \quad (4)$$

In the equations above, *N* refers to the number of expected load effect events in the extrapolated return period, which is estimated from linearly extrapolating the number of events found in the time for which the WIM data were collected. Note that because the WIM equipment cannot capture some traffic patterns, and in particular, trains of slow moving vehicles that are closely spaced, it is possible that actual load effects may be underreported in the projections.

This process is repeated for each WIM site and each load effect, which are span-dependent. As the design calibration is desired to be conducted independent of bridge location within the state, the final load effect statistics $\bar{L}_{\max}$ and $\sigma_{L\max}$ used for a particular load effect, span, lane load (1-lane or 2-lane), and bridge type are then taken as the mean of those determined from the different WIM sites for the particular case considered.

In this study, loads are distributed to girders using the AASHTO LRFD girder distribution factor (DF) expressions. A complication arises in that there is no DF equation in AASHTO LRFD that accounts for vehicles in two lanes of different weights and configurations. A technique such as finite element analysis or grillage modeling would be ideal in this case. However, the time involved to construct detailed numerical models for each of the many different bridge configurations considered is not feasible. Therefore, an approximate method is used, as suggested by Moses (2001). Here, the total two-lane load effect (M_{12}) is given by:

$$M_{12} = M_1 DF_1 + M_2(DF_2 - DF_1) \quad (5)$$

In this expression, M_1 is the load effect due to the vehicle(s) in lane 1; DF_1 is the AASHTO LRFD single lane DF (after removing the multiple presence factor of 1.2); M_2 is the load effect due to the vehicle(s) in lane 2 (while in the recorded spatial position on the span relative to the lane 1 vehicle, per the WIM data); and DF_2 is the AASHTO LRFD 2-lane DF. The AASHTO DF formula are known to be generally conservative when compared to actual distribution factors found from bridge field studies (see for example, Nowak et al. 2000; Eamon et al. 2014b, among many others). A significant contributor to this discrepancy has been shown to stem from the presence stiffening elements such as barriers, sidewalks, and diaphragms that are not accounted for in the DF formula (Eamon and Nowak 2002), although the additional load distribution benefits that these elements provide may not be reliable in the case of an overload causing girder failure. Although the uncertainty in DF resulting from the use of the AASHTO LRFD formula has been considered in the model as described in more detail below, the use of these expressions may be regarded as conservative.

An example normal projection line is given in Figure 5. As noted above, the load projection is based on the assumption that the original tail well-fits a normal distribution, where goodness of fit is indicated with a straight line on the normal probability plot. It was found that the vast majority of the upper tail of load effect data could be well-fit by linear regression, with nearly all coefficients of determination (R^2) above 0.95, and the majority in the range of 0.98 and above.

For comparison, Figures 6a-d present mean maximum load effect projections for 2 years and at 75 years. As expected, the mean maximum values are above the mean values (of the top 5% of load effects used to develop the mean maximums) given in Figure 4. Also note that the single maximums shown in Figure 3 are significantly above the mean maximums in most cases.

This is also expected, as the single maximum represents the largest values within the range of load effects used to develop the mean maximum. As shown, the mean maximum projections result in very similar curves as shown for the top 5% load effects given in Figure 4. This is not surprising, given that the top 5% of the data are well-fit by the projection model, as discussed above. However, note that the curve shapes given by the 2 year mean maximum projections do not exactly match the shapes of the curves formed from the top 5% of load data (which are also based on 2 years of data). This is so for several reasons. The top 5% of load effects shown in Figure 4 are made from the top load effects from all WIM sites taken together, whereas to be meaningful, the projected load effects are developed on a site-specific basis, then the site-averaged projections are presented, so the results are weighted somewhat differently. However, the main reason that the curve shapes are different is that differences in coefficient of variation (COV) exist for different load effects and spans. This changing variance is not captured in the top 5% graph, but strongly affects the projections, where, as variance increases, so does the projected load effect. This variance tends to magnify differences in mean load effects and spread results further apart when mean maximums are projected.

Once the mean maximum 75-year base live load effects on the girder are determined, the results are multiplied by the mean dynamic load allowance (IM) to produce the mean maximum total live load to the girder, $\overline{LL}_{max}$. For heavy vehicles, mean IM is taken as 1.15 for the single lane case and 1.10 for two-lanes loaded (Nowak 1999).

The above process determines the mean maximum live load effect on a girder. To determine COV of maximum live load on the girder, V_{LLmax}, several uncertainties are considered beyond that from the data projection (V_{proj}), as suggested by Sivakumar et al. (2011); geographic location (V_{site}); the WIM data at a particular site (V_{data}); dynamic load allowance (V_{IM}); and load

distribution to the girder (V_{DF}). V_{proj} is found directly from the results of the data projection (i.e. $V_{proj} = \sigma_{L\max} / \bar{L}_{\max}$), while V_{site} is computed directly as the COV of $\bar{L}_{\max}$ values found from the different sites. There is no direct way to assess V_{data}. However, Sivakumar et al. (2011) suggests that it is estimated based on a standard deviation taken equal to the value of data at the 95% upper and lower confidence intervals. In this study, it was found that V_{data} was below 2% for all cases investigated and did not significantly contribute to live load COV. V_{IM} is taken as 9% for 1-lane effects and 5.5% for 2-lane effects, while values for V_{DF} are given in Table 7, which were determined from a statistical analysis of experimental results determined from actual bridge structures as compared to those predicted by the AASHTO DF expressions (Sivakumar and Ghosn 2011).

For a product function of random variables (RVs) such as girder load effect, if the RVs are uncorrelated and COV is reasonably small, then COV of the function can be reasonably determined by ignoring the second order relationships to estimate V_{LLmax} as:

$$V_{LLmax} = (V_{proj}^2 + V_{site}^2 + V_{data}^2 + V_{IM}^2 + V_{DF}^2)^{1/2} \quad (6)$$

The resulting statistics are shown in Table 8, where the 75-year mean maximum and COV of the live load L_{max} used in this study are compared to those used in the AASHTO LRFD calibration (prior to reduction by DF or application of IM), In the table, "MI/LRFD" is the ratio of the mean values of $\bar{L}_{\max}$ (at 75 years) used in this study to that used in the AASHTO LRFD calibration. As shown in the table, mean maximum values are significantly higher than those used to calibrate the AASHTO LRFD code, where ratios ranged from 1.3-2.1.

Additional load random variables include dead loads from prefabricated components (D_p), site-cast components (D_s), and the wearing surface (D_w), with statistics taken from Nowak (1999) and given in Table 9. Similarly, statistical parameters for girder resistance R are taken

from Nowak (1999) to be consistent with the AASHTO LRFD and MBE calibrations, and are also shown in Table 9. Mean resistance $\overline{R}$ is calculated from $\overline{R} = R_n \lambda_r$. Here, R_n is the nominal resistance, given by AASHTO LRFD, and λ_r is bias factor.

Reliability Analysis

Reliability for each bridge can then be calculated. Once load RVs are converted to load effects applied to the girder, the general limit state function is:

$$g = R - (D_p + D_s + D_W) - LL_{max} \quad (7)$$

In the AASHTO LRFD design calibration, for reliability analysis, girder resistance was taken as a lognormal random variable while the sum of load effects was assumed normal. This simplification is used in this study as well for consistency. In the calibration process, it is desired to determine the required vehicular live load factor (γ_L) needed to achieve reliability results closest to the LRFD target of β=3.5. Due to the large number of reliability calculations required, the reliability analysis is conducted with the closed form, simplified First Order, Second Moment (FOSM) procedure, such that the required γ_L can be solved for directly. With algebraic manipulation, the FOSM approach can be rewritten to allow solution of the live load factor directly using the quadratic equation with the following coefficients (Eamon et al. 2014):

$$A = R_L^2 - \beta^2 V_R^2 R_L^2$$

$$B = 2R_L R_D - 2\overline{Q} R_L - 2\beta^2 V_R^2 R_L R_D$$

$$C = R_D^2 - 2\overline{Q} R_D - \beta^2 V_R^2 R_D^2 + \overline{Q}^2 - \beta^2 \sigma_Q^2 \quad (8)$$

where R_L = vehicular design live load effect on the girder, not including the live load factor; R_D = design dead load effect on the girder, including the load factors (i.e. 1.25DC+1.5DW); V_R = COV of resistance; $\overline{Q}$ = mean total load effect; σ_Q = standard deviation of total load effect; and

β = the desired target reliability index. In this process, only the maximum (1.25DC) Strength I and II dead load factor was considered; use of other dead load factors (such as those from Strength IV) is beyond the scope of the calibration. However, the 0.9 minimum DC factor, as well as the Strength IV limit state, did not govern the design of the structures considered in this study. Note that the calibration is conducted assuming that the bridge is designed according to current LRFD procedures (for example, using the sectional design model for shear analysis, rather than the shear design method presented in the Standard Specifications).

The FOSM method used assumes all RVs are normal, which is conservative when resistance is lognormal, as assumed for bridge member resistance. To develop a more accurate assessment of reliability and minimize this conservatism, a series of Monte Carlo Simulations (MCS) were conducted on a selection of cases considered in the calibration resulting from the limit state function shown in eq. 7. In each case, the corresponding reliability index resulting from $1x10^7$ MCS runs, β_{MCS}, was considered to be the "exact" solution. This value was then compared to the reliability index determined from the FOSM procedure, β_{FOSM}. For a target reliability index of β=3.5, it was found that the ratio of $\beta_{MCS} / \beta_{FOSM}$ varied narrowly for the problems considered in this study, from about 1.06-1.08. Therefore, for use in the calibration, the reliability index was taken as $\beta = 1.07\beta_{FOSM}$.

Results

The live load factor for each bridge type considered is taken as the maximum required from the single or two lane loaded case. Note all results are given for the standard AASHTO LRFD HL-93 design load, not MDOT's LRFDmod design load. In general, two-lane effects tended to govern in the following cases: simple moments for 6, 30, and 61 m (20, 100, and 200

ft) spans; simple shears for 6 and 15 m (20 and 50 ft) spans; and continuous moments for 6, 15, and 61 m (20, 50, and 200 ft) spans. This occurs due to the interaction of multiple factors. Of these, a significant factor is the differing dominant vehicle pattern for 1-lane and 2-lane load effects, as discussed earlier, where one pattern tends to govern over another as span length changes. However, several other factors influence which case dominates as well. Two additional primary factors include changing proportional differences in the 1- and 2-lane distribution factors as span changes, and differences in load effect variability (COV of load effect changes with span and number of lanes loaded, affecting girder reliability). Overall, however, single lane load effects (i.e. with following vehicles) governed more frequently than two-lane effects. This indicates that in Michigan, for many bridge spans, a greater probability exists for experiencing an overload from truck(s) in a single lane rather than from side-by-side trucks. There is significant variability in γ_L, which considering up to 61 m (200 ft) spans, ranges from a maximum of 3.83 (side-by-side box beam in simple shear, 61 m span) to a minimum of 1.25 (spread box beams, 3.7 m (12 ft) spacing, 6 m (20 ft) span in continuous shear). The variability primarily results from discrepancies between the HL-93 design load effect and the actual load effect on the structures.

For most cases, the required load factor increases as girder spacing decreases, and occurs whether a single lane load effect or a two lane load effect governs. Considering the case when the single lane governs, it can be shown that the ratio of the single lane DF to the AASHTO two-lane DF used for design increases as girder spacing decreases, as shown in Figure 7 (leftmost graph). Thus, the proportion of actual load effect (based on the 1-lane DF) to the design load effect (based on the two-lane DF for a two lane bridge) similarly increases. For the case when the two-lane load effect governs, a similar trend occurs, where the ratio of the actual two-lane load

effect to the load effect determined from the AASHTO two-lane DF used for design increases as girder spacing decreases. This is because the AASHTO DF design formula assumes two trucks of equal weight in both lanes, but in the vast majority of cases, the WIM data revealed that the vehicle(s) in lane 1 (typically the rightmost lane) has a much greater load effect than the vehicle(s) in the adjacent lane. Moreover, the proportion of load distributed to the governing girder from lane 1 to lane 2 increases as girder spacing decreases. This latter trend is shown in Figure 7 (rightmost graph), which provides the ratio of the factors in eq. 5 used to proportion load effects from lane 2 (DF2 – DF1) to that of lane 1 (DF1) to the girder. As shown, as girder spacing decreases, proportionally less load effect is developed from lane 2.

A selection of required load factors for specific cases is given in Figures 8-11. In Figures 8 and 9, which present results for composite steel and spaced box beam girders, respectively, for each span, a group of 5 load factors are given, in order, for girder spacings of 1.2, 1.8, 2.4, 3.1, and 3.7 m (4, 6, 8, 10, and 12 ft). For composite steel girders, load factors ranged from 1.25 (continuous shear, 6 m (20 ft) span, 3.7 m (12 ft) girder spacing) to 3.50 (simple shear, 61 m (200 ft) span, 1.2 m (4 ft) girder spacing), with a mean of 2.27. For prestressed concrete girders, load factors ranged from 1.29 (continuous shear, 6 m span, 3.7 m girder spacing) to 3.80 (simple shear, 6 m span, 1.2 m girder spacing), with a mean of 2.29. Results for prestressed concrete are nearly identical to those of composite steel, and thus a separate figure is not provided for brevity. Figure 9 provides results for spaced box beams, where load factors ranged from 1.25 (continuous shear, 6 m span, 3.7 m girder spacing) to 3.60 (simple shear, 61 m span, 1.2 m girder spacing), with mean of 2.28.

Figure 10 shows side-by-side box beam results. In the figure, for each load effect, a group of 6 load factors are computed in order for spans of 6, 15, 24, 31, and 61 m (20, 50, 80,

100, and 200 ft). Results are shown for two values of box beam stiffness for each span (low and high), which ranged from 900 mm (36 in) to greater than 1500 mm (60 in) deep, depending on span. As seen, box beam stiffness has minimal effect on required load factor. In Figure 10, load factors ranged from 1.69 (continuous shear, 6 m (20 ft) span) to 3.83 (simple shear, 61 m (200 ft) span), with a mean of 2.59.

In Figure 11, results are presented for long span structures of 92 and 122 m (300 and 400 ft). These spans are generally achieved with unique structural components and systems rather than standard bridge girders. However, for long span results to be widely useful, the calibration is not conducted for a unique structure, but rather developed to be applicable to any non-specific structural component. The procedure used is the same as that considered for girder bridges, but with two exceptions. First, dead load is determined based an assumed proportion of dead load-to-live load effect to the component (DL/LL) rather than directly computed. That is, the design live load effect is first computed for the span, then dead load effect is determined by multiplying the live load effect by an assumed DL/LL ratio. Second, no girder distribution factor is applied to the live load effect, as it is not applicable for non-girder bridges. In this case, the assumed DL/LL ratio implicitly includes the effect of the structural analysis procedure used to proportion dead and live load effect to the component. Based on a survey of large span structures, DL/LL load effect ratios of 1.5, 2.25, and 3.0 for moment and 2.0, 3.0, and 4.0 for shear effects were considered. These ratios refer to unfactored dead load to HL-93 live load (with dead load effect proportions for D_w, D_p, and D_s of approximately 0.14, 0.52, and 0.34, respectively, proportions which are usually significantly different for shorter spans). This represents a general procedure applicable to any generic bridge member. It provides identical results to the girder bridge reliability analysis for the same DL/LL load effect ratios, if the same DF is used in design as well

as the reliability analysis. For each load effect in Figure 11, a group of 6 load factors is given, where the first three correspond to 92 m spans with the DL/LL ratios of 1.5, 2.25, and 3.0 for moment and 2.0, 3.0, and 4.0 for shear effects, while the next three load factor results correspond to 122 m spans with the same load proportions.

As seen in the figure, when 92-122 m spans are considered, higher load factors are required as compared to shorter spans, with an average of 2.48 for composite steel components and 2.90 for prestressed concrete components. This significant increase over the shorter span average is not due to the HL-93 design load inaccurately modeling the load effect at longer spans; in fact, the HL-93 model becomes more conservative as span length increases beyond 61 m (200 ft) as compared to the measured load effects. Rather, the increase relative to the 6-91 m (20-200 ft) spans is primarily due to the DL/LL effect ratio, which is significantly larger than that for shorter spans. For example, the average DL/LL ratio for all load effects for composite steel girders was approximately 0.98 (compared to the range of DL/LL of 1.5-3.0 for the long span structures considered). As this ratio increases, a higher proportion of the nominal load effect is factored with a lower load factor for design, an effect which is not effectively counter-balanced by the associated decrease in COV of load effect as dead load proportion increases for longer spans. Note that for the shorter span bridges, the changing proportion of DL/LL is appropriately accounted for, as the HL-93 design load model and accompanying load factors were developed for these typical shorter span (i.e. less than 61 m) DL/LL proportions.

Although the maximum live load factors for the worst case bridges appear large, results are not unexpected. As noted earlier, completely legal, non-permit Michigan trucks configurations may exceed 710 kN (160 kips) GVW, far in excess of the 356 kN (80 kip) federal limit, and result in a database of relatively high routine traffic load effects to calibrate to. Even

so, the resulting load factor results are not that unusual when compared to some findings elsewhere. For example, based on WIM data from several states, NCHRP 683 presents approximate maximum live load factors ranging from about 3.1-3.8 for spans up to 61 m, values similar to the maximum live load factors determined in this study. Similarly, with regard to average load factor, it was found that in Florida that the live load factor required an increase to 2.37 to meet a target reliability index of 3.5 (Sivakumar et al. 2011), which is within the range of the mean values reported above.

Conclusions and Recommendations

In this study, a reliability-based calibration of design live load factors specific to the State of Michigan was conducted. Using vehicle weight and configuration filtering criteria developed for the project, high frequency WIM data from 20 Michigan sites were collected. Load effects were generated for bridge spans from 6 to 122 m (20 to 400 ft) considering simple and continuous moments and shears, as well as single lane and two lane effects, then projected to 75 years. Bridge structures considered for the calibration included composite steel, prestressed concrete, reinforced concrete, and box beam girder bridges, as well as special long span structures. Significant variation was found in the live load factors required to meet a target reliability index of 3.5.

Several levels of recommendation are given below, with different trade-offs with respect to ease of use and consistency in safety level. The most accurate approach would be to use the particular live load factor found for each type of bridge girder considered, as shown in Figures 8-11. This would produce theoretically uniform levels of reliability for girders, such that all considered structures exactly meet the target reliability level of 3.5. The use of different load

factors for different bridge types and geometries may appear cumbersome for many designers. However, this type of approach is not new to MDOT engineers, who currently use a similar system of multiple load factors. For example, at present, 25 different vehicle configurations are combined with three different weight classes, to produce a table of 75 live load factors that are used for bridge rating (MDOT 2009). In this context, the use of a similar system for bridge design is not unreasonable.

As a more traditional alternative, a simplified version of the above can be developed, of which multiple reasonable approaches are possible. A very conservative approach would be to impose a minimum load factor γ_L necessary for any bridge to meet β=3.5; this would result in a load factor of approximately 3.6 for steel and PC girder structures, about 3.8 for box beams, and 4.0 for long span structures. However, as these very high load factors only apply to a few specific cases out of the hundreds considered, the large majority of structures would be greatly overdesigned, and thus this approach is not recommended. A less conservative possibility is to base load factor on an average results. For example, if the cases shown in the figures are counted such that steel, PC, and spread box beam girder bridges are each weighted at about 30%, while side-by-side box beam bridges are weighted at 10%, to approximate proportions of existing and expected future types of structures as suggested by MDOT, then the mean load factor required is 2.3, just slightly higher than the minimum current MDOT effective load factor of 2.1. This approach may work well if the variation in load factor is not too large. However, such a greatly simplified approach is not recommended in this case, since a large variation in safety level is present, and many structures will have reliability indexes between 2 and 3.

As a compromise between the two extremes above, a still relatively simple approach may be devised by using a reduced set of load factors applied to similar groups of structures, while

impose two main constraints: that the average reliability index for all structures must be no less than 3.5, and also that a minimum acceptable reliability index is maintained for any possible case. This minimum acceptable level will depend on the needs of the agency. For this study, a reasonable allowance of variation in reliability index is suggested such that β_{min} =3.0 is allowed for any individual girder. The resulting load factor framework could then be structured as follows:

For spans up to 61 m (200 ft):

For moment, γ_L = 2.5

For shear, γ_L =3.2

For long spans:

For moment, γ_L = 2.2

For steel structures in shear, γ_L = 3.0

For PC structures in shear, γ_L =3.8

The above system produces an average reliability index of 4.2 for spans up to 200 ft, while for longer spans, average reliability index is 3.8, where no individual girder has reliability index less than 3.0 (note the large discrepancy in load factor between long span steel and PC structures in shear, as well as the differences shown in Figure 11. This is a result of the higher COV of PC shear resistance, as shown in Table 11, an effect which is masked by the dominance of other uncertainties associated with the higher live to dead load ratios of lower spans). Certainly, other LF schemes are possible as well. When considering load factors for the longer spans, it should be again noted that the current Michigan WIM systems cannot accurately capture situations where vehicles are slow moving and closely spaced. As such a traffic pattern may govern load

effects, this issue should be revisited in the future when such an investigation of Michigan traffic becomes possible.

A comparison of this simplified load factor scheme to the existing effective load factors developed by using the current LRFDmod design load is shown in Figure 12. It can be see that the ratio of proposed/HL-93 load factor is about 20% higher than the existing HL93-mod/HL-93 load factor for moment for spans greater than about 20m (65 ft), but is substantially lower than the existing HL93-mod/HL-93 ratio for shorter spans. For the longest spans, however, greater than 91m (300 ft) the proposed and existing load factors closely match. For shear, the HL93-mod/HL-93 load factor ratio exceeds the proposed/HL-93 ratio only for spans less than about 9m (30 ft), where for longer spans, the proposed/HL-93 ratio exceeds the existing by about 50% on average.

In summary, a multiple load factors approach where each structural type has its own load factor is ideally recommended, but if deemed impractically cumbersome, then a simplified system such as that described above, where the average reliability level of girders is at the target level, while none are below a minimum level such as 3.0, for example, may be feasible.

Finally, it should be noted that better consistency in safety level can likely be achieved by adjusting the design load model, as was done previously by MDOT. This is because various qualitative differences were found between the LRFD and Michigan calibration results, such as the single lane load effect in Michigan often governs over the two lane effect; that shear effects worsen at longer spans and smaller girder spacing; and that short continuous spans have inconsistently high reliability as compared to other spans, for example. Due to the complex nature of the inconsistency of the results, however, a reliability based design optimization (RBDO) procedure is recommended to guide design load model development. Typically, RBDO

is applied to select the physical characteristics of a structure to optimize performance under reliability-based constraints (see for example Thompson et al. 2006), but the same concept can be applied to the load model itself that is used to design the structure. In this approach, an optimum notional design vehicle configuration is developed such that when applied, inconsistencies in reliability among different types of structures are minimized. Such an optimized load model may allow the use of a simple load factor system, or perhaps even a single live load factor, to provide reasonable consistency in safety level. Such an approach is recommended for future research.

Acknowledgements

The authors wish to thank the Michigan Department of Transportation Research Administration for support of this effort.

References

AASHTO (1994). “LRFD Bridge Design Specifications,” American Association of State Highway and Transportation Officials, Washington, D.C.

AASHTO (2011). "Manual for Bridge Evaluation," American Association of State Highway and Transportation Officials, Washington, D.C.

Ang, A. and Tang, W. (2007) "Probability Concepts in Engineering: Emphasis on Applications to Civil and Environmental Engineering," 2nd Ed., John Wiley and Sons.

Bruls A, Croce P, Sanpaolesi L, and Sedlacek O. (1996). "ENV1991 - Part 3: Traffic Loads on Bridges; Calibration of Load Models for Road Bridges." Proceedings, IABSE Colloquium, Delft, 439-53.

Croce P., and Salvatore W. (2001). "Stochastic Model for Multilane Traffic Effects on Bridges." *ASCE Journal of Bridge Engineering*, 6(2), 136-143.

Curtis, R. and Till, R. (2008). "Recommendations for Michigan Specific Load and Resistance Factor Design Loads and Load and Resistance Factor Rating Procedures." MOOT Research Report R-1511.

Eamon, C., and Nowak, A.S. (2002). “Effects of Edge-Stiffening Elements and Diaphragms on Bridge Resistance and Load Distribution,” *ASCE Journal of Bridge Engineering,* 7(5), 258-266.

Eamon, C., Kamjoo, V., and Shinki, K. (2014). "Side by Side Probability for Bridge Design and Analysis." MDOT Report RC-1601.

Eamon, C., Parra-Montesinos, G., and Chehab, A. (2014b). "Evaluation of Prestressed Concrete Beams in Shear." MDOT Report RC-1615.

Fu, O. and Van de Lindt, J. (2006). "LRFD Load Calibration for State of Michigan Trunkline

Bridges." MDOT Research Report RC-1466.

FHWA (2001). "Traffic Monitoring Guide." FWHA-PL-Ot-021. Federal Highway Administration, Washington, D.C.

Ghosn, M., Sivakumar, B., and Miao, F. (2011). "Load and Resistance Factor Rating (LRFR) in NYS, Volume II, Final Report." NYSDOT Report C-06-13.

Gindy, M., and Nassif, H.H. (2007). "Multiple Presence Statistics for Bridge Live Load Based on Weigh-In-Motion Data." *Transportation Research Record*, 2028, 125-135.

Kwon, O-S, Kim, E., Orton, S, Salim, H., and Hazlett, T. (2010). "Calibration of the Live Load Factor in LRFD Design Guidelines", MODOT Report ORI1-003, 2010.

Lee, C.E. and Souny-Slitine, N. (1998). "Final Research Findings on Traffic-Load Forecasting Using Weight-in-Motion Data." Center for Transportation Research Bureau of Engineering Research, the University of Texas at Austin, Report 987-7.

"MDOT Bridge Analysis Guide, 2005 Ed., with 2009 Interim Update, Parts 1 and 2." (2009). Michigan Department of Transportation Construction and Technology Support Area, Lansing, MI.

Monsere, L., Higgins, C. and Nichols, A. (2011). "Application of WIM Data for Improved Modeling, Design, and Rating." Oregon Transportation Research and Education Consortium, Oregon Department of Transportation.

Moses, F. (2001). "Calibration of Load Factors for LRFR Bridge Evaluation." NCHRP Report 454, Transportation Research Board, Washington, D.C.

Nowak, A.S. (1999). "Calibration of LRFD Bridge Design Code", NCHRP Report 368, Transportation Research Board, Washington, D.C.

Nowak, A.S., Sanli, A., and Eom, J. (2000). "Development of a Guide for Evaluation of Existing Bridges Phase 2." MDOT Report RC-1378.

O'Brien, E. and Caprani, C. (2005). "Headway Modeling for Traffic Load Assessment of Short to Medium Span Bridges." *The Structural Engineer*, 83(16), 33-36.

O'Brien, E. and Enright, B. (2011). "Modeling Same-Direction Two-Lane Traffic for Bridge Loading." *Structural Safety*, 33, 296-304.

O'Brien, E. Enright, B., and Getacllew, A. (2010). "Importance of the Tail in Truck Weight Modeling for Bridge Assessment." *ASCE Journal of Bridge Engineering*, 15(2), 210-213.

O'Connor A, Jacob B, O'Brien E, and Prat M. (2001). "Report of Current Studies Performed on Normal Load Model of ECL Part 2. Traffic Loads On Bridges." *Revue Francaise de Genie Civil*. 5(4), 411-433.

Pelphrey, J. and Higgins, C. "Calibration of LRFR Live Load Factors Using Weigh-In-Motion Data, Interim Report SPR 635, June, 2006.

Pelphery, J., Higgins, CH., Sivakumar, B., Groff, R.L., Hartman, B.H., Charbonneau, J.P., Rooper, J.W., and Johnson, B.V. (2008). "State-Specific LRFR Live Load Factors Using Weigh-in-Motion Data." *ASCE Journal of Bridge Engineering*, 13(4), 339-350.

Raz, O., Buchheit, R., Shaw, M., Koopman, P., and Faloutsos, C. (2004). "Detecting Semantic Anomalies in Truck Weigh-In-Motion Traffic Data Using Data Mining." A*SCE Journal of Computing in Civil Engineering*, 18(4), 291-300.

Sivakumar, B., Ghosn, M., and Moses, F. (2011). "Protocols for Collecting and Using Traffic Data in Bridge Design." NCHRP Report 683, Transportation Research Board, Washington, D.C.

Sivakumar, B. and Ghosn, M. (2011). “Recalibration of LRFR Live Load Factors in the AASHTO Manual for Bridge Evaluation.” NCHRP Project 20-07, Task 285.

Tabatabai, H., Zhao, J., and Lee, C-W. (2009). "Statistical Analysis of Heavy Truck Loads Using Wisconsin Weigh-In-Motion Data." WDOT Project CFIRE 01-02.

Thompson, M., Eamon, C., and Rais-Rohani, M. (2006) “Reliability-Based Optimization of Fiber-Reinforced Polymer Composite Bridge Deck Panels,” *ASCE Journal of Structural Engineering*, 132(12), 1898-1906.

Van de Lindt, J. and Fu, G. (2002). "Investigation of the Adequacy of Current Bridge Design Loads in the State of Michigan." MDOT Research Report RC-1413.

List of Tables

List of Figures

Table 1. WIM Data Filtering Criteria.

Check	Criteria for Elimination*	% Eliminated**
GVW	GVW < 53	19%
	$(GVW - \Sigma W_A)/GVW > 0.10$	
Axle Wt. (W_A)	($W_{A\ first\ axle}$) < 27 or ($W_{A\ first\ axle}$) > 111	56%
	($W_{A\ any\ axle}$) < 9 or ($W_{A\ any\ axle}$) > 312	
Axle Spacing (S)	$S_{first\ axle} < 1.5$	50%
	$S_{any\ axle} < 1.0$	
Speed (V)	V < 30 or V > 160 for GVW < 890	1.4%
	V < 30 or V > 140 for GVW > 890	
No. of Axles (n)	n < 2 or n > 13	<0.0001%

*Units for weight and spacing in kN and m. Speed units in kph **Some vehicles were eliminated by multiple criteria, hence elimination percentage sums greater than 100%.

Table 2. Summary of Vehicle GVW (kN) By Site

	Mean				Mean		
Site	All	Top 5%	Max	Site	All	Top 5%	Max
400A	235	583	1210	5000A	254	562	2190
400B	260	574	1120	5000B	252	518	1760
1000A	269	648	1220	5000C	253	580	2420
1000B	255	709	1466	5000D	250	490	1200
1000C	251	665	2270	5000E	237	360	1260
1000D	269	663	1210	5000F	246	617	1470
1000E	230	631	1190	5000G	249	490	1250
2500A	248	630	1420	5000H	237	599	1390
2500B	254	523	1200	5000I	207	550	1640
2500C	249	585	1250	5000J	258	565	1950

Table 3. Side-by-Side Probabilities Based on WIM Data (%).

	Vehicle Headway (m)					
ADTT	3	6	12	24	48	1/2 TL
<1000	0.04	0.04	0.04	0.04	0.06	0.04
1000-2500	0.17	0.21	0.32	0.56	0.97	0.24
2500-5000	0.40	0.55	0.93	1.73	3.13	0.65
>5000	0.68	0.97	1.62	3.04	5.61	1.18

Table 4. Other Multiple Presence Probabilities Based on WIM Data (%).

	Span (m)				
	6	18	31	55	122
ADTT <1000					
Following	0.03	0.06	0.08	0.10	0.18
Multiple	0.02	0.02	0.02	0.03	0.03
1000<ADTT<2500					
Following	0.38	0.74	0.98	1.12	2.40
Multiple	0.05	0.07	0.09	0.11	0.14
2500<ADTT<5000					
Following	1.61	2.38	3.21	4.06	4.72
Multiple	0.18	0.35	0.48	0.58	0.97
ADTT>5000					
Following	3.58	4.41	7.28	7.87	8.93
Multiple	0.65	1.12	1.63	1.87	2.11

Table 5. Summary of Load Effects on Bridge Span Based on WIM Data.

	Moment (kN-m)				Shear (kN)			
Span (m)	Mean	COV	Min.	Max.	Mean	COV	Min.	Max.
Single Lane (Following), Simple Span								
6	126	0.35	38	975	98	0.38	22	703
31	1240	0.44	192	9640	165	0.46	45	1100
122	8090	0.49	763	53300	240	0.52	85	2800
Single Lane (Following), Continuous Span								
6	94	0.38	8	452	98	0.36	27	552
31	559	0.47	20	1800	165	0.43	45	1320
122	2500	0.53	154	24600	245	0.52	53	2780
Two Lane, Simple Span								
6	53	0.38	5	679	36	0.44	4	547
31	338	0.42	37	3850	80	0.44	9	1080
122	14900	0.41	1190	130000	481	0.41	40	4300
Two Lane, Continuous Span								
6	35	0.42	4	369	36	0.40	4	441
31	258	0.41	22	2250	71	0.50	4	1010
122	6460	0.41	497	54100	449	0.41	40	4130

Table 6. Single Vehicle and Following Load Effects on Bridge Span Based on WIM Data.

Span (m)	Mean	COV	Min.	Max.
Simple Span Moment, Single Vehicles (kN-m)				
6	126	0.35	38	843
15	431	0.39	97	3340
31	1220	0.44	192	8010
61	3090	0.43	386	17400
92	4960	0.43	578	26800
122	6830	0.43	763	36200
Simple Span Moment, Single and Following Vehicles				
6	126	0.35	38	975
15	432	0.39	97	3670
31	1240	0.44	192	9640
61	3470	0.44	386	25000
92	5770	0.47	578	39800
122	8090	0.49	763	53300

Table 7. Coefficient of Variation for Girder Distribution Factor.

Bridge Type	Moment		Shear	
	1 Lane	2 Lane	1 Lane	2 Lane
Composite Steel	0.11	0.14	0.14	0.18
PC	0.12	0.13	0.11	0.16

*From Sivakumar and Ghosn (2011).

Table 8. 75-Year Mean Maximum Live Load Statistics on Bridge Span.

Span (m)	Moment (kN-m)	COV	MI/LRFD*	Shear (kN)	COV	MI/LRFD*
Simple Spans						
6	532	0.18	1.30	392	0.19	1.39
15	2570	0.24	1.72	668	0.20	1.64
24	5670	0.27	1.90	877	0.21	1.74
31	7874	0.26	1.90	988	0.21	1.79
61	22600	0.21	2.07	1450	0.22	2.11
Continuous Spans						
6	386	0.17	1.44	392	0.19	n/a
15	1690	0.19	1.79	663	0.20	n/a
24	3820	0.22	1.68	872	0.21	n/a
31	5000	0.20	1.60	979	0.21	n/a
61	10500	0.21	1.21	1440	0.21	n/a

Single lane values are provided prior to reduction by DF for consistent comparison; 2-lane values have higher values overall, but are not listed as they do not govern in most cases after DF is applied.
*COV of live load effect for AASHTO LRFD was taken as 0.18-0.20 for all spans. The LRFD load effect used for calibration was not provided for continuous shears.

Table 9. Random Variable Statistics*.

Random Variable		Bias Factor	COV
Resistance RVs	R		
Prestressed Concrete, Moment		1.05	0.075
Prestressed Concrete, Shear		1.15	0.14
Composite Steel, Moment		1.12	0.10
Composite Steel, Shear		1.14	0.105
Load RVs			
Vehicle Live Load	LL_{max}	varies	
DL, Prefabricated	D_p	1.03	0.08
DL, Site-Cast	D_s	1.05	0.10
DL, Wearing Surface	D_w	mean 89 mm	0.25

*From Nowak (1999), with the exception of LL_{max}, which was determined in this study.

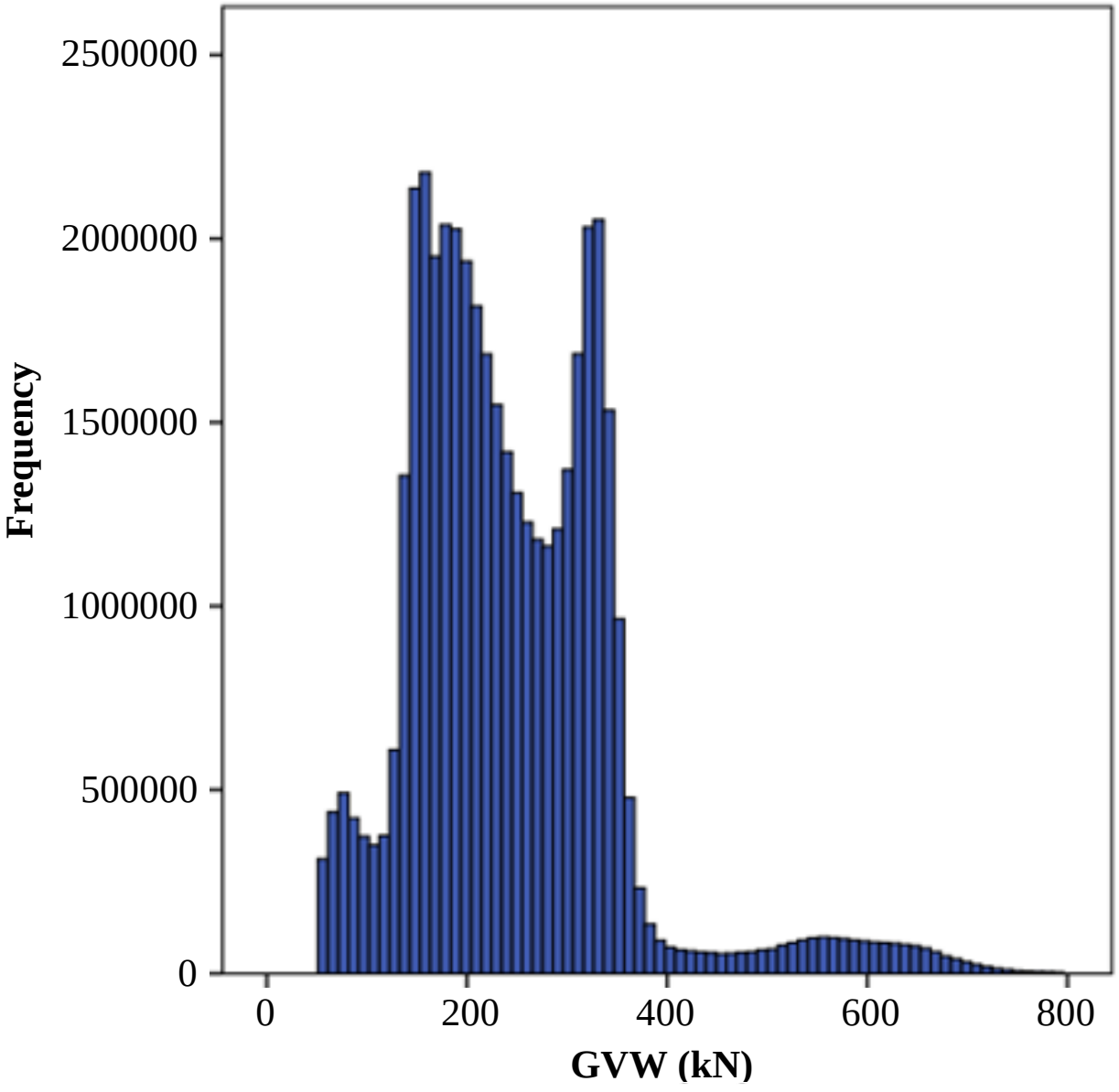

Figure 1. Frequency Histogram for All Vehicles Based on WIM Data.

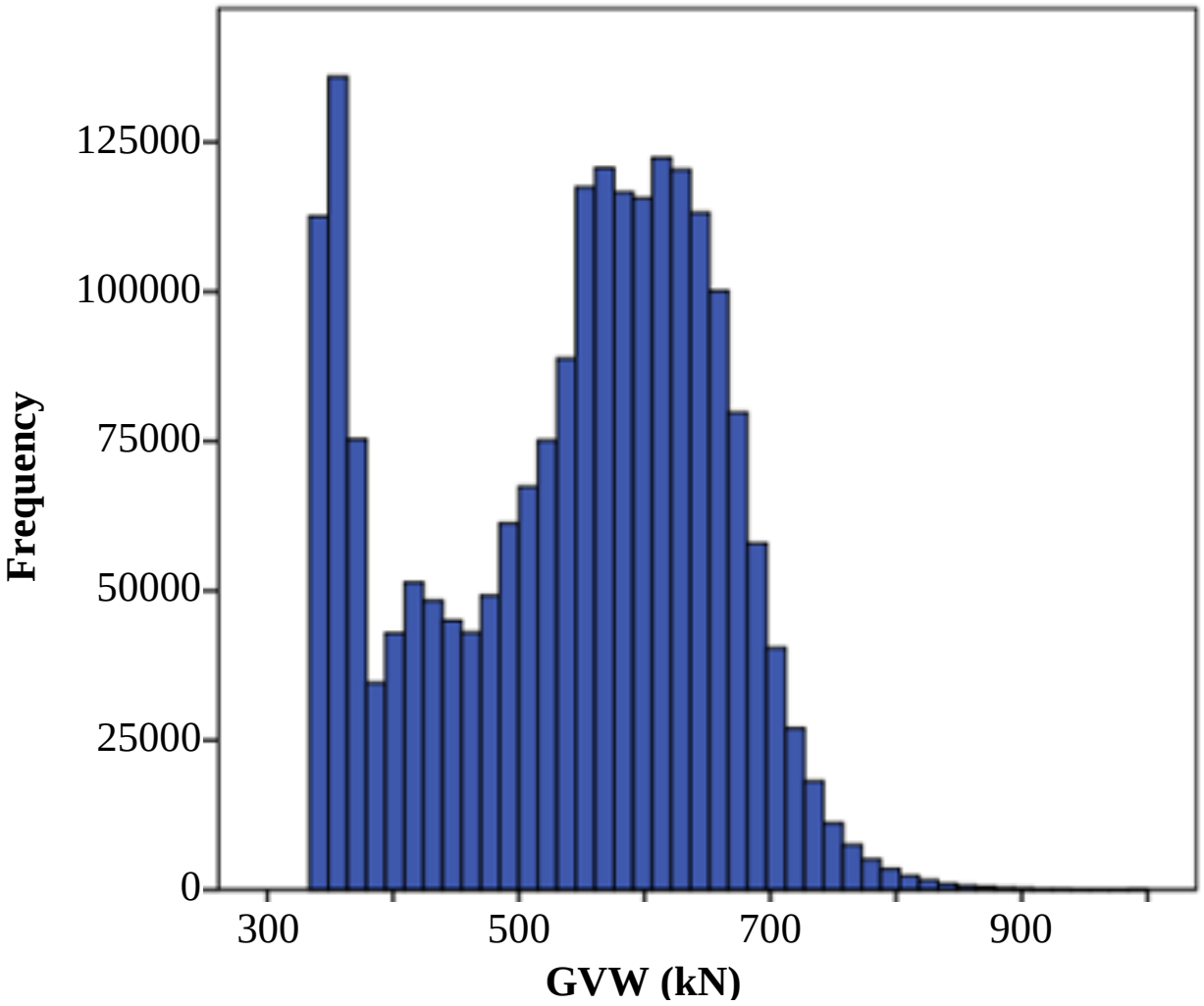

Figure 2. Frequency Histogram for Top 5% of Vehicles Based on WIM Data.

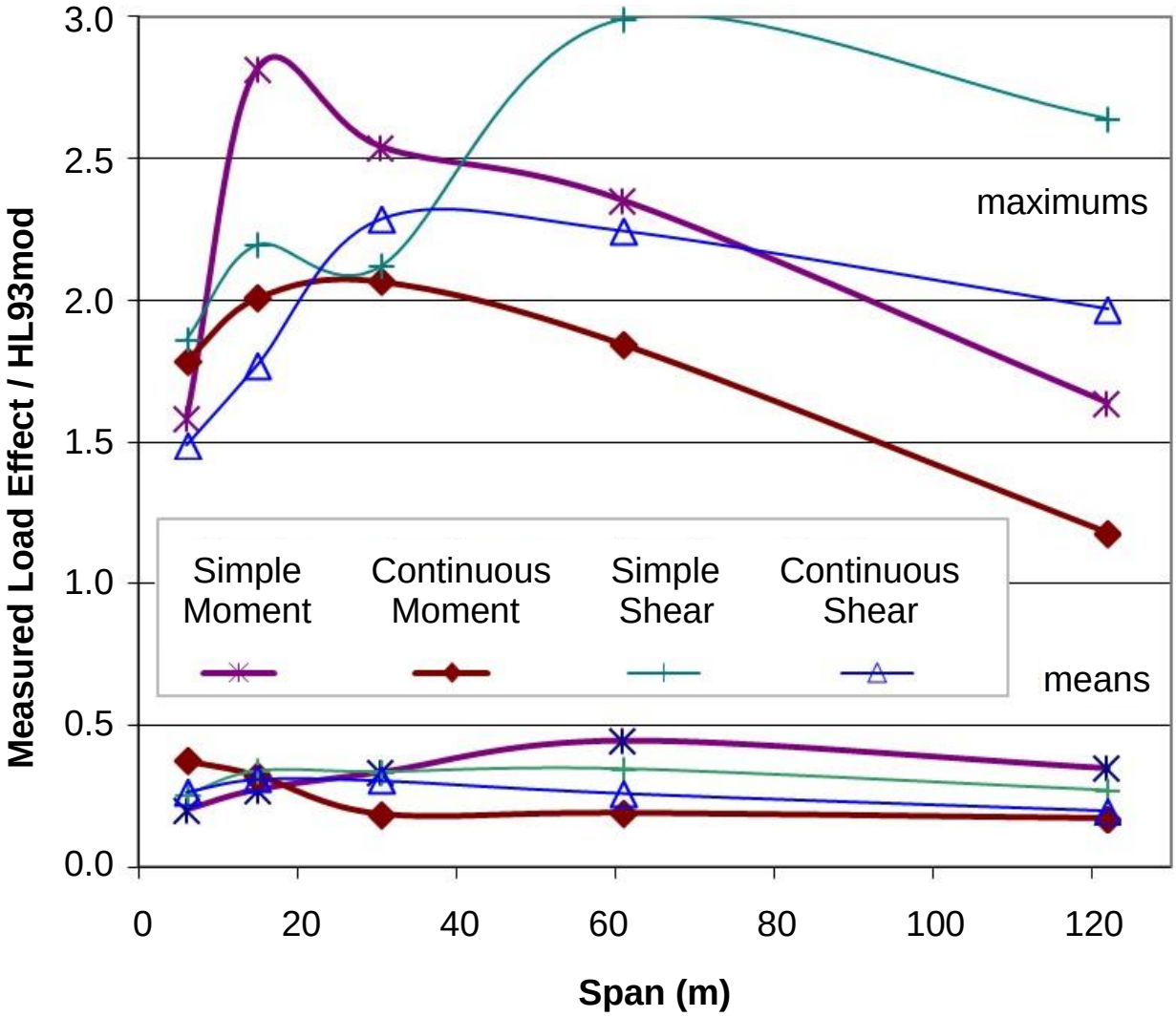

Figure 3. Single Maximum and Mean Ratios of Measured Load Effects to Existing Unfactored HL93mod Load Effect.

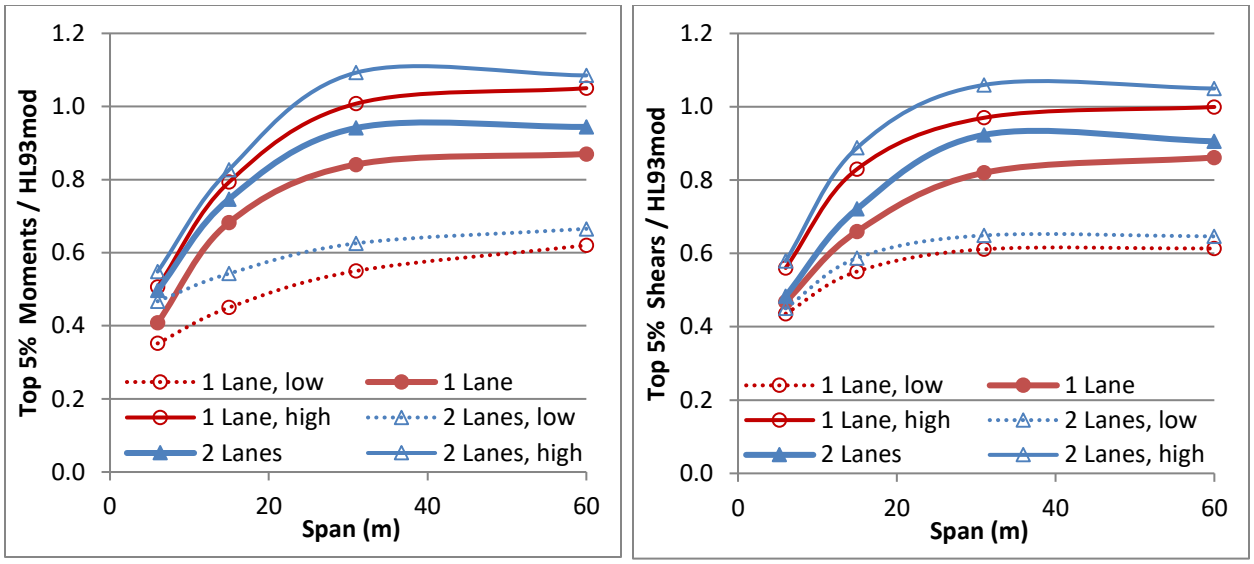

(a) (b)

Figure 4. Ratios of Top 5% Simple Moments (a) and Shears (b) to HL93-mod.

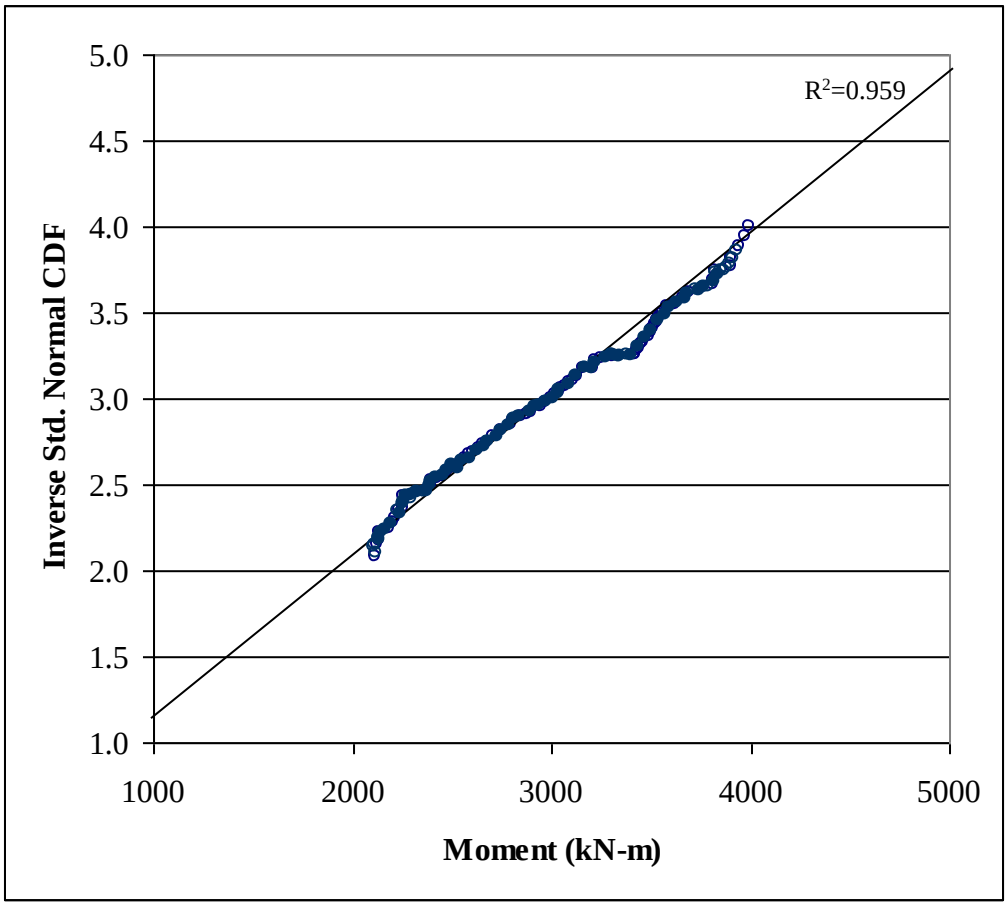

Figure 5. Example of Normal Fit of Top 5% of Single Lane Simple Moments Used for 75 Year Projection, Based on WIM Data, 24 m Span.

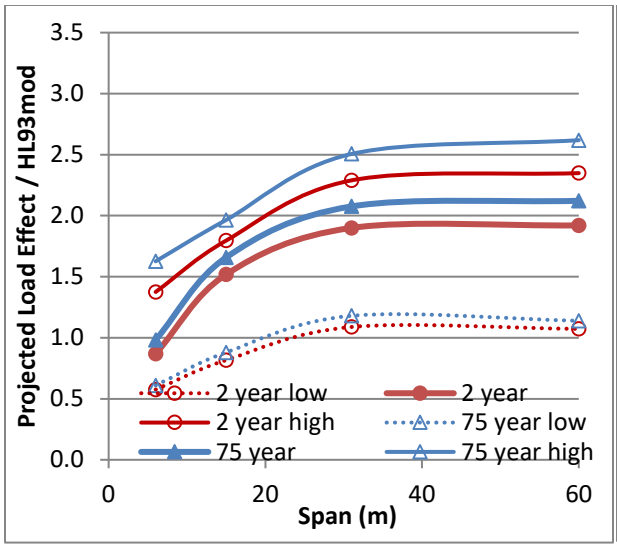

Figure 6a. Simple Moments, 1 Lane.

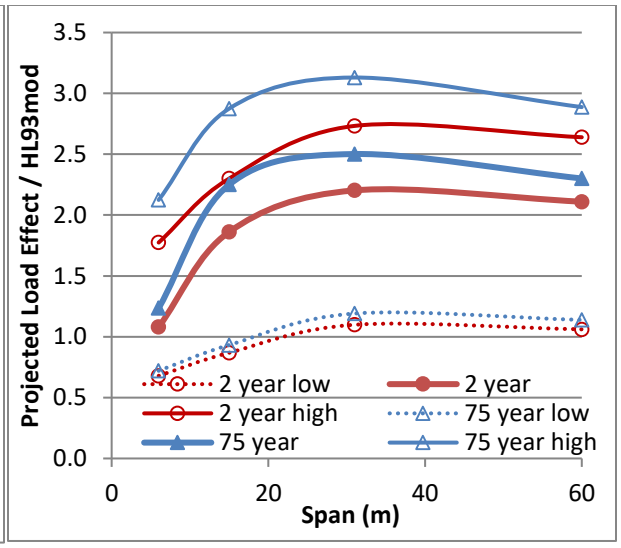

Figure 6b. Simple Moments, 2 Lanes.

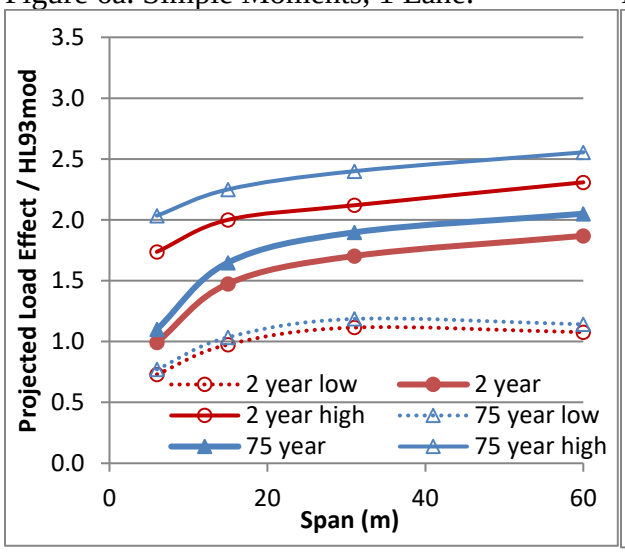

Figure 6c. Simple Shears, 1 Lane.

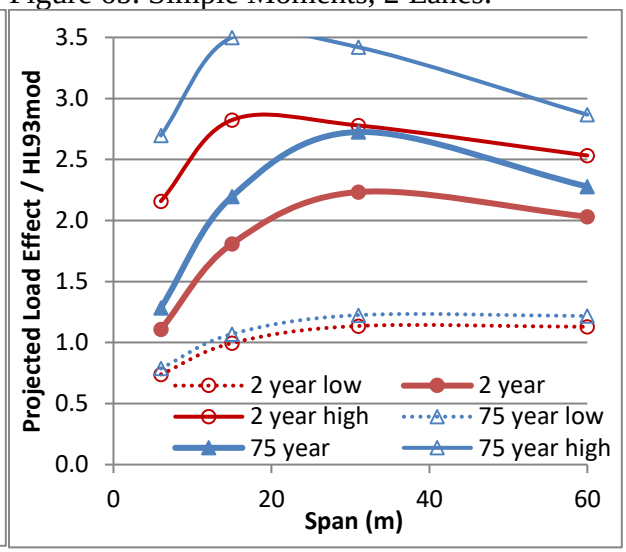

Figure 6d. Simple Shears, 2 Lanes.

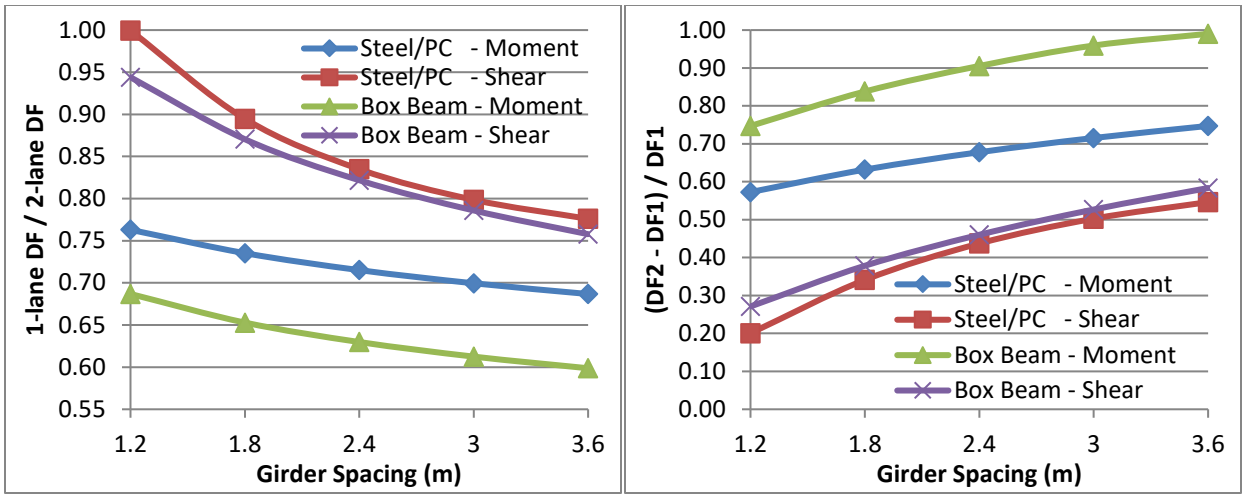

Values are given for an example 24 m (80 ft) span, but trends remain unchanged for all spans considered.

Figure 7. Distribution Factor Ratios.

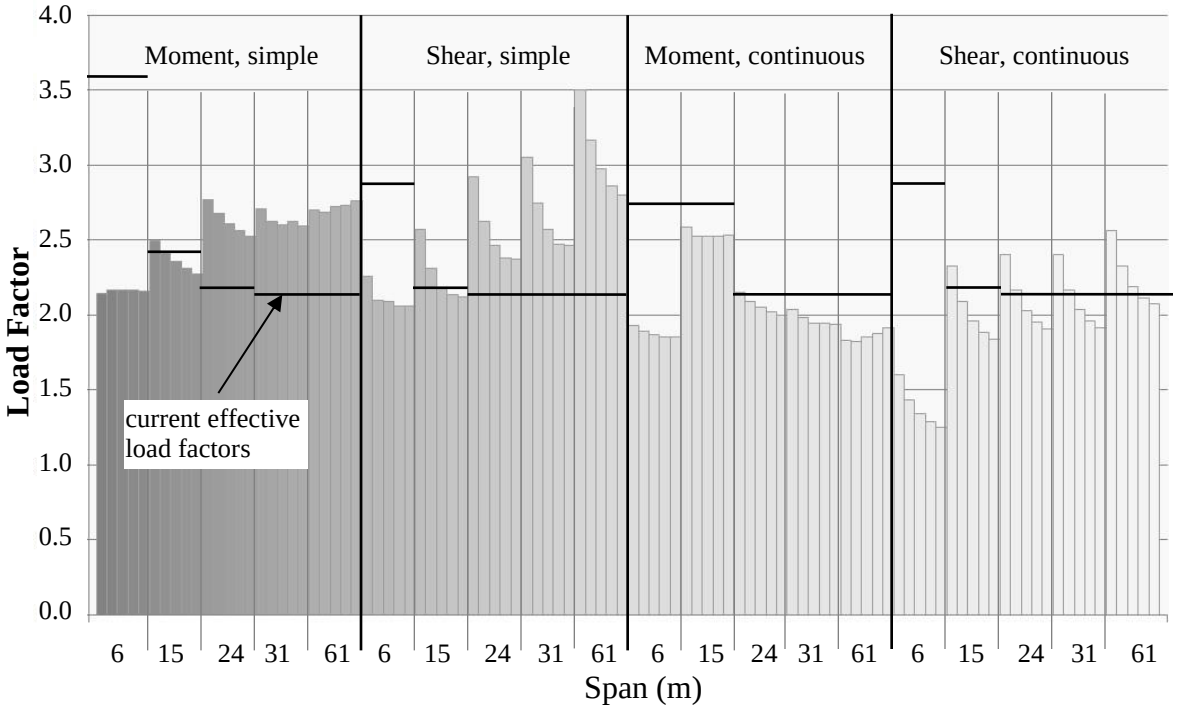

Figure 8. Load Factors for Composite Steel Girders Needed to Meet β=3.5.

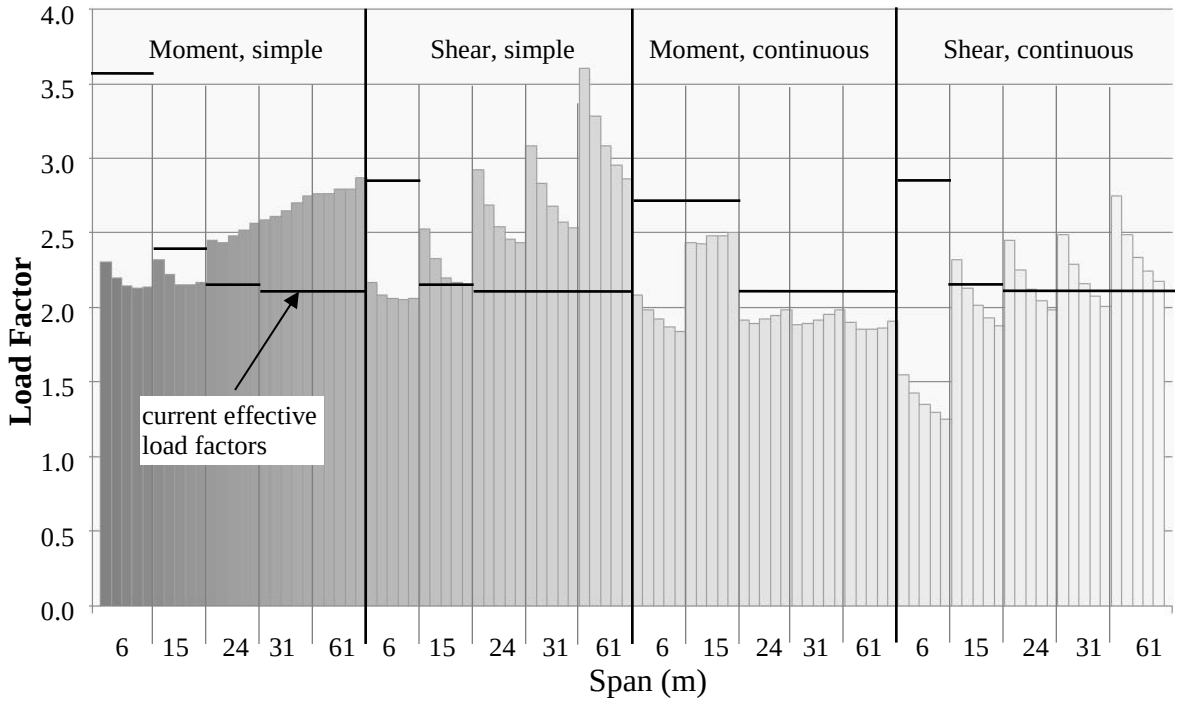

Figure 9. Load Factors for Spaced Box Beams Needed to Meet β=3.5.

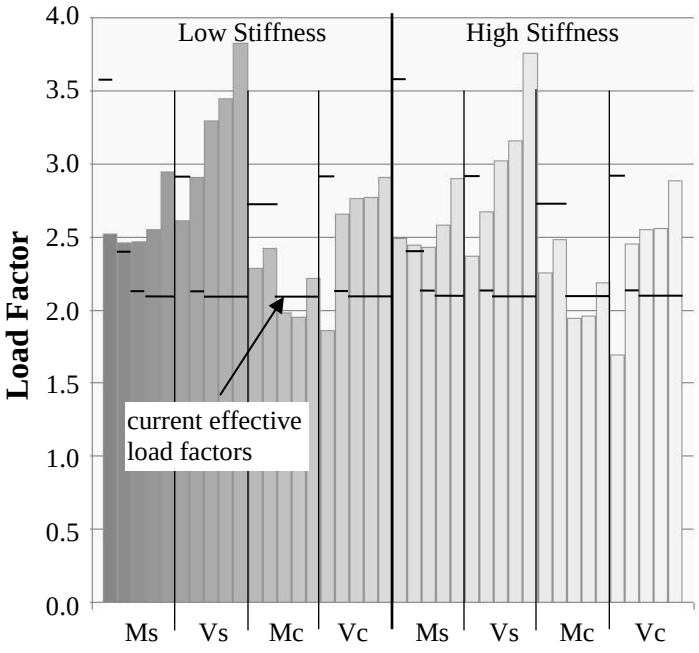

Figure 10. Load Factors for Side-By-Side Box Beams Needed to Meet β=3.5.

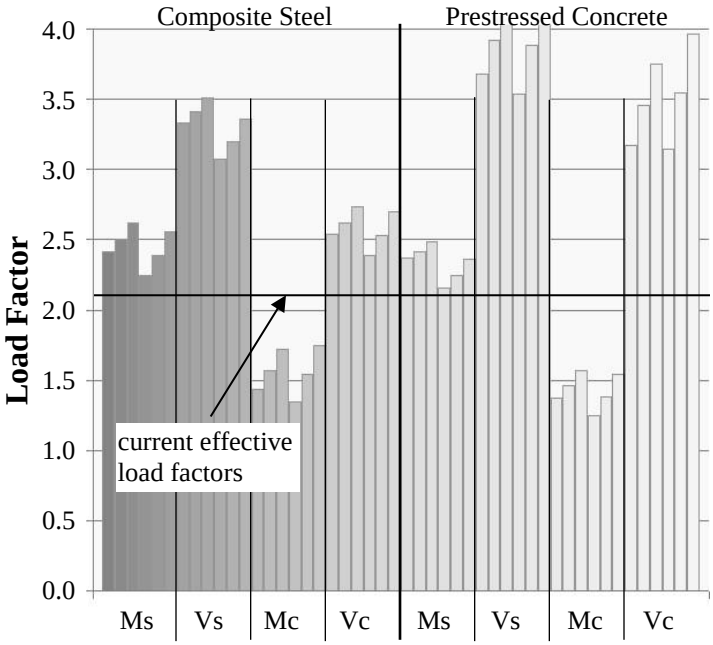

Figure 11. Load Factors for Long Span Structures Needed to Meet β=3.5.

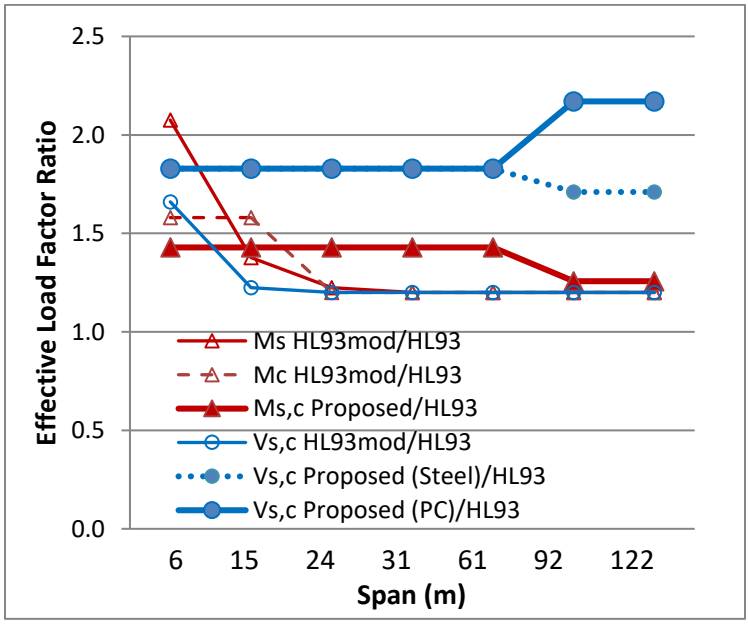

Ms: simple moment; Mc: continuous moment; Ms,c: both moments;
Vs,c: simple and continuous shears

Figure 12. Comparison of Existing and Proposed (Simplified) Live Load Factor Ratios.